

Article

# Novel Mechanism of SIRT3 Regulation in Cardiac Inflammatory Injury: The Key Role of MITOL

Ping Li<sup>1</sup>, Lingzhi Wang<sup>1,\*</sup>

<sup>1</sup>Department of Paediatrics, Zhang Ye People's Hospital affiliated to Hexi University, 734000 Zhangye, Gansu, China

\*Correspondence: [13830601230@163.com](mailto:13830601230@163.com) (Lingzhi Wang)

Submitted: 1 February 2024 Revised: 27 March 2024 Accepted: 10 April 2024 Published: 19 June 2024

## Abstract

**Background:** Myocardial injury is a common heart disease that involves various forms of cell death, including pyroptosis. Lipopolysaccharide (LPS) can simulate the inflammatory response of cardiomyocytes, resulting in their damage. Sirtuin 3 (SIRT3), a mitochondrial deacetylase, has been shown to play a role in cardiac protection. This study aimed to investigate whether SIRT3 mitigates inflammation-induced cardiomyocyte pyroptosis and alleviates LPS-induced myocardial injury via the mitochondrial ubiquitin ligase (MITOL)-dependent mechanism. **Methods:** Mouse and H9C2 cardiomyocyte models were used to simulate myocardial inflammatory injury by LPS treatment. Cardiac ultrasound, protein expression analysis, mRNA expression detection, and serum biochemical indicators were used to assess the extent of myocardial injury. The EdU experiment was conducted to detect cell proliferation capacity. DCFH-DA fluorescence was used to measure Reactive Oxygen Species (ROS) levels. JC-1 probe analysis was used to assess the aggregate/monomer ratio in different treatment groups. Furthermore, SIRT3 treatment and MITOL silencing experiments were conducted to explore the impact of SIRT3 on cardiomyocyte pyroptosis and whether it functions through MITOL. Scanning electron microscopy experiments were conducted to assess the reversal of the protective effect of SIRT3 by silencing MITOL. **Results:** The experimental results showed that LPS treatment significantly impaired mouse cardiac function, increased the expression of pyroptosis-related proteins in cardiomyocytes, elevated serum myocardial injury indicators, and increased the mRNA expression of inflammatory factors (tumor necrosis factor- $\alpha$  (TNF $\alpha$ ) and interleukin-1 $\beta$  (IL-1 $\beta$ )). SIRT3 treatment significantly reduced LPS-induced myocardial injury, improved cardiac function, reduced the expression of pyroptosis-related proteins, and decreased inflammatory factors. Silencing MITOL reversed the protective effect of SIRT3 on cardiomyocyte injury, suggesting that SIRT3 exerted its therapeutic effect through MITOL. **Conclusion:** This study revealed that SIRT3 mitigated inflammation-induced cardiomyocyte pyroptosis via a MITOL-dependent mechanism, thereby alleviating LPS-induced myocardial injury. This finding pro-

vides a new molecular target for the treatment of myocardial inflammation-related diseases and lays a theoretical foundation for the development of cardiac protection strategies. Future research can further explore the potential application of the SIRT3-MITOL axis in cardiac diseases, providing effective treatment methods for cardiac patients.

## Keywords

myocardial injury; SIRT3; inflammation; pyroptosis; mitochondrial ubiquitin ligase pathway

## Introduction

Cardiac inflammation is an important pathological process leading to myocardial cell damage and cardiac dysfunction. Researchers have long recognized that the lipopolysaccharide (LPS)-induced cardiac cell inflammatory response can lead to myocardial cell pyroptosis, exacerbating myocardial injury [1–3]. Sirtuin 3 (SIRT3), as a mitochondrial deacetylase, has been shown to protect myocardial cells from oxidative stress and apoptosis damage through multiple mechanisms [4–6]. However, how SIRT3 regulates pyroptosis of myocardial cells under inflammatory conditions remains unclear, particularly through the mechanism of mitochondrial ubiquitin ligase (MITOL) [7].

In recent years, the role of mitochondria in cardiomyocytes has become a focus of cardiology research [8,9]. Mitochondria are not only the center of cellular energy metabolism but also a crucial organelle in regulating cell death [10,11]. The role of SIRT3 in cardiac protection has been gradually revealed, inhibiting programmed cell death of myocardial cells by regulating antioxidant defense and energy metabolism within the mitochondria [12,13]. SIRT3 can alleviate oxidative stress by activating antioxidant enzymes [14–16]. MITOL has recently been found to play a significant role in regulating mitochondrial morphology and function, and it plays a critical role in maintaining mitochondrial network stability [17–20]. However, reports on the interaction between SIRT3 and MITOL and their functions in myocardial cell inflammation remain limited.

Despite the attention given to the roles of SIRT3 and MITOL in cardiac protection, their specific interaction mechanisms in myocardial cell pyroptosis remain unclear. Under inflammatory conditions, whether SIRT3 can regulate myocardial cell pyroptosis through MITOL and the molecular mechanisms of this process are areas lacking research. The role and potential therapeutic value of the SIRT3-MITOL axis in LPS-induced myocardial injury need further exploration.

This study aimed to investigate the role of SIRT3 in mitigating inflammation-induced myocardial cell pyroptosis through a MITOL-dependent mechanism, as well as determine the significance of this process in alleviating LPS-induced myocardial injury. Using cellular and animal models, this study comprehensively investigated the regulatory role of SIRT3 on MITOL and how this regulation affects the survival of myocardial cells under inflammatory conditions. Through these investigations, we hope to reveal the molecular mechanism of the SIRT3-MITOL axis in myocardial cell pyroptosis, providing new targets for the treatment of cardiac inflammation-related diseases. Additionally, the findings of this study may contribute to the development of new cardiac protection strategies, offering effective treatment methods for cardiac patients.

## Methods

### *LPS-Induced Mouse Myocardial Injury Animal Model*

Twenty-four 8-week-old male C57BL/6 mice were purchased from GemPharmatech Biotechnology Co., Ltd. (Jiangsu, China). The animals were housed in an SPF-level environment with a temperature of  $20\text{ }^{\circ}\text{C} \pm 2\text{ }^{\circ}\text{C}$ , humidity of 40%–70%, and a 12-hour light–dark cycle. All experimental animal procedures and housing conditions complied with the regulations of the Experimental Animal Center and animal ethics. The *Sirt3* sequence (NM\_022433.2) was obtained from Gene Bank. SIRT3 lentivirus overexpression vector was constructed in OBiO Technology (Shanghai) Corp., Ltd. Lentivirus ( $20\text{ }\mu\text{L}$ ,  $1 \times 10^8\text{ Tu/mL}$ ) was injected into the anterior wall of the left ventricle by using an insulin syringe. Sepsis-related cardiac dysfunction was induced by injecting LPS (Sigma-Aldrich, St. Louis, MO, USA) at a dose of  $10\text{ mg/kg}$  for 12 h, as previously described [21]. The blank control group was injected with an equivalent amount of saline (IN9000, Solarbio, Beijing, China). Mice were anesthetized with 4% pentobarbital sodium ( $10\text{ mg/kg}$ ) (P1020, Solarbio, Beijing, China), blood was collected from the eyeball, and the mice were euthanized. The heart tissues were quickly removed, washed, and divided into two parts. One part was rapidly frozen in liquid nitrogen and stored at  $-80\text{ }^{\circ}\text{C}$  for later use. The other part was fixed in paraformaldehyde (P1110, Solarbio, Beijing, China), embedded in paraffin, and sectioned. The col-

lected blood was left at  $4\text{ }^{\circ}\text{C}$  for 2 h and centrifuged at 3000 rpm for 10 min, and the supernatant was collected for further use. This study was approved by the Ethics Committee of Zhang Ye People's Hospital affiliated to Hexi University (Approval No. ZYAF/SQ-02/02.1).

### *Assessment of Cardiac Function by Echocardiography*

The Vevo2100 small animal ultrasound imaging system (VisualSonics, Toronto, Ontario, Canada) was used to assess cardiac function. The left ventricular papillary muscle horizontal short-axis and long-axis sections were selected, and the left ventricular ejection fraction (EF) and fractional shortening (FS) of the mice were measured and recorded using a high-frequency ultrasound diagnostic instrument (30 MHz frequency).

### *Western Blot*

After weighing the myocardial tissues, they were transferred to a grinder, and 1 mL of RIPA lysis buffer (containing 1 mmol/L protease inhibitor (P6730, Solarbio, Beijing, China)) (R0010, Solarbio, Beijing, China) was added per 0.1 g of tissue. The tissues were ground and lysed on ice. The supernatant was collected after centrifugation at 14,000 rpm for 30 min, and the protein concentration in the supernatant was measured using the BCA (PC0020, Solarbio, Beijing, China) method. The samples were denatured by boiling in protein loading buffer (D1060, Solarbio, Beijing, China) and then stored at  $-80\text{ }^{\circ}\text{C}$ . SDS-PAGE gels (P1200, Solarbio, Beijing, China) were prepared, and  $10\text{ }\mu\text{g}$  of total protein was loaded into each well. After electrophoresis and band separation, the proteins on the gel were transferred to a PVDF membrane (YA1701, Solarbio, Beijing, China). The PVDF membrane was blocked with 5% skim milk (D8340, Solarbio, Beijing, China) in TBST (T1081, Solarbio, Beijing, China) for 2 h, washed, and incubated with primary antibodies against SIRT3 ([D22A3] Rabbit mAb #5490, 1:1000, ab217319, Abcam, Cambridge, UK), MITOL (Antibody #19168, 1:1000, ab188029, Abcam, Cambridge, UK), Caspase-1 (#2225, CST, 1:1000, ab207802, Abcam, Cambridge, UK), NLRP3 (Rabbit mAb #15101, 1:1000, ab263899, Abcam, Cambridge, UK), IL-1 $\beta$  (#12242, 1:1000, ab283818, Abcam, Cambridge, UK), and GSDMD (Rabbit mAb #39754, 1:1000, ab219800, Abcam, Cambridge, UK) at  $4\text{ }^{\circ}\text{C}$  for 12 h. After washing the bands with TBST and TBS (T1080, Solarbio, Beijing, China), they were incubated with secondary antibodies (goat anti-rabbit (ab288151, Abcam, Cambridge, UK) at 1:5000 or goat anti-mouse (ab150115, Abcam, Cambridge, UK) at 1:3000) at room temperature for 2 h. The goat anti-rabbit IgG-HRP and goat anti-mouse IgG-HRP were purchased from Santa Cruz, USA. The bands were washed with TBST and TBS and then visualized using ECL luminescent reagent (32209, Thermo Scientific, Waltham, Massachusetts, USA). The grayscale values of the bands were

calculated using ImageJ software (version 1.5f, National Institutes of Health, Maryland, USA), with GAPDH (1:1000, ab8245, Abcam, Cambridge, UK) as the internal reference.

#### qRT-PCR

The myocardial tissue was ground in TRIzol (R1100, Solarbio, Beijing, China), and total RNA was extracted according to the extraction process instructions. The purity and concentration were measured by using a spectrophotometer (UV-1900, Shimadzu, Tokyo, Japan). Reverse transcription (K1691, Solarbio, Beijing, China) and qPCR (T2210, Solarbio, Beijing, China) were performed according to the instructions of the reverse transcription and qPCR kits, and the relative levels of the inflammatory factors interleukin-6 (IL-6) and tumor necrosis factor- $\alpha$  (TNF- $\alpha$ ) in mouse myocardial tissue were calculated. The primer sequences were as follows: IL-6 (F: 5'-CTGCAAGAGACTTCCATC-CAG-3', R: 5'-AGTGCTATAGACAGGTCTGTTGG-3'); TNF- $\alpha$  (F: 5'-CCTCTAGCCCACGTCGTAG-3', R: 5'-GGGAGTAGACAAGCTACAACCC-3'); GAPDH (F: 5'-TGGCCTCCGTGTTCCCTAC-3', R: 5'-GAGTTGCTGTTGAAGTCGCA-3').

#### ELISA

After cardiac function assessment, blood was collected from the eyeball of the mice, centrifuged at 3000 rpm for 15 min at 4 °C, and the serum was separated and stored at -80 °C. Lactate dehydrogenase (LDH), creatine kinase-MB (CK-MB) activity, and cardiac troponin I (cTnI) levels in mouse serum were determined according to the kit instructions. Standard samples in the enzyme-linked immunosorbent assay (ELISA) kit were diluted to different concentrations to create a standard curve. LDH (m1002267) and CK-MB (ml037723) ELISA kits were purchased from Shanghai Enzyme-linked Biotechnology Co., Ltd. The cTnI (E-EL-M1805) ELISA kit was purchased from Shanghai Boyao Biotechnology Co., Ltd.

#### HE Staining

The paraffin-embedded tissue was cut into consecutive coronal sections (4  $\mu$ m). The sections were deparaffinized in xylene, rehydrated in a graded series of ethanol, and stained with hematoxylin for 4 min and eosin for 2 min. The HE staining kit (G1120) was purchased from Beijing Solarbio Company. Pathological changes in myocardial tissue were observed under an optical microscope (CX23, Olympus, Tokyo, Japan), and images were captured using a microscope digital camera (DS-Fi3, Nikon, Tokyo, Japan).

#### TUNEL Staining

Paraffin-embedded sections of myocardial tissue were deparaffinized in xylene (X8010, Solarbio, Beijing, China), rehydrated in graded ethanol (C0161S, Beyotime, Shanghai, China), and incubated with 100 mg/mL proteinase K (ST533, Beyotime, Shanghai, China) at 37 °C for 30 min, followed by 10 min of incubation with 3% hydrogen peroxide (ST858, Beyotime, Shanghai, China). These sections were incubated with the terminal deoxynucleotidyl transferase dUTP nick end labeling (TUNEL) reaction mixture at 37 °C for 1 h, followed by three washes with PBS (C0221A, Beyotime, Shanghai, China). The TUNEL kit (T2190) was purchased from Beijing Solarbio Company. The cell nuclei were stained with DAPI solution (C1002, Beyotime, Shanghai, China) for 5 min. After washing three times with PBS, the sections were observed under a fluorescence microscope (IX83, Olympus, Tokyo, Japan). The apoptotic rate was calculated as the number of apoptotic cells (green) divided by the total number of cells (blue) multiplied by 100%.

#### H9C2 Cell Culture and Transfection

H9C2 (iCell-r012, Cellverse Bioscience Technology Co., Ltd., Shanghai, China) rat cardiomyocytes were seeded in culture flasks containing 90% DMEM, 10% fetal bovine serum (Gibco, Life Technologies, Rockville, MD, USA), and 1% penicillin-streptomycin (iCell-15140-122, Cellverse Bioscience Technology Co., Ltd., Shanghai, China) at 37 °C with 5% CO<sub>2</sub>. In all subsequent experiments, the cells were stimulated with 5  $\mu$ g/mL LPS. The H9C2 cells were grouped and treated according to the experimental requirements. The cell lines used in this study have undergone mycoplasma testing and STR identification. The mimics of MITOL small interfering RNA (siRNA) and SIRT3 overexpression plasmid (pCMV-SIRT3 and pCMV-NC) were synthesized by GenePharma (Shanghai, China). Cell transfection was carried out using the Lipofectamine 3000 kit (L3000001, Thermo Fisher Scientific, Shanghai, China). MITOL siRNA1, sense: 5'-GGUGCAGAGGAUCUACUAATT-3', antisense: 5'-UUAGUAGAUCUCUGCACCTT-3'; MITOL siRNA2, sense: 5'-GCAGGUUGUAGGCCAUAAATT-3', antisense: 5'-UUUAUGGCCUACAACCUGCTT-3'; MITOL siRNA3, sense: 5'-CCAGCUGAAGCUAACCCUUTT-3', antisense: 5'-AAGGGUUAGCUUCAGCUGGTT-3'. siRNA-NC: sense: 5'-UUCUCCGAACGUGUCACG UTT-3', antisense: 5'-ACGUGACACGUUCGGAGA ATT-3'.

#### CCK-8 Assay

H9C2 cells were evenly seeded in a culture plate and subjected to different treatments. After a designated incubation period, CCK-8 reagent was added, and the cells

were incubated to metabolize CCK-8 (CA1210, Solarbio, Beijing, China) into a yellow product. Finally, data were obtained by measuring absorbance, typically at a wavelength of 450 nm, using an ELISA reader (Multiskan Sky Microplate Spectrophotometer, Thermo Fisher Scientific, Wilmington, MA, USA).

#### *DCFH-DA Fluorescence Detection of ROS Levels*

The ROS levels in myocardial cells were determined using the DCFH-DA fluorescent probe. The DCFH-DA fluorescent probes were purchased from Beijing Solaibao Technology Co., Ltd. H9C2 cells were seeded in a 6-well plate and treated with LPS after 24 h. Following the respective operation manuals, the corresponding detection working solution was added, and the cells were incubated at 37 °C for 30 min, followed by washing the cells twice. Finally, myocardial cell ROS was observed under a fluorescence microscope. Changes in ROS were indicated by changes in green fluorescence intensity.

#### *JC-1 Probe Detection*

The mitochondrial membrane potential was detected using the JC-1 fluorescent probe. The JC-1 staining kit was purchased from Beyotime Company (Cat# C2005, Shanghai, China). About 180  $\mu$ L of prepared staining working solution was added to the treated cells. The levels of mitochondrial membrane potential were indicated by the ratio of JC-1 aggregates (excitation and emission wavelengths of 525 and 590 nm, respectively) to JC-1 monomers (excitation and emission wavelengths of 490 and 530 nm, respectively) by using a fluorescence microplate reader (TriStar<sup>2</sup> S, Berthold Technologies, Baden-baden, Germany).

#### *Scanning Electron Microscopy Experiment*

Cells were plated in a 6-well plate with clean cover slips. When the cells reached 50%–80% confluence, they were washed three times with PBS (pH 7.4). The cover slips were removed, washed with PBS, fixed with 2.5% glutaraldehyde (P1126, Solarbio, Beijing, China) for 30 min, and washed three times with PBS. Subsequently, they were fixed with 1% osmium tetroxide (20816-12-0, TCI, Tokyo, Japan) for 30 min and washed three times with PBS. Dehydration was performed sequentially with 50%, 70%, and 90% anhydrous ethanol (C0161S, Beyotime, Shanghai, China). The samples were then immersed in a mixture of anhydrous ethanol and isoamyl acetate (123-92-2, MACKLIN, Beijing, China), followed by immersion in pure isoamyl acetate and left overnight at 4 °C. The glass slides with specimens were fixed on copper specimen holders using conductive paste, dried to the critical point, and sputter-coated with platinum for observation and photography using a Hitachi S-3000N scanning electron microscope (Tokyo, Japan).

#### *Statistical Analysis*

SPSS 20.0 software (SPSS Inc., Chicago, IL, USA) was used for data analysis, and the experimental results were expressed as mean  $\pm$  standard deviation. One-way ANOVA was used for comparisons between multiple groups, and the *t*-test was used for comparisons between two groups. A *p*-value less than 0.05 was considered statistically significant.

## **Results**

#### *LPS Induced Myocardial Injury in Mice*

According to the results of left ventricular ejection fraction (LVEF) and left ventricular end-systolic volume (LVFS), LPS treatment significantly reduced cardiac pumping function; the higher the dosage, the more severe the impact (Fig. 1A,B). At the protein expression level (Fig. 1C), LPS treatment increased the expression of MITOL, Caspase-1, and NLRP3 (Fig. 1D–F), indicating that LPS induced mitochondrial and inflammatory stress. Meanwhile, the expression of SIRT3 decreased in the LPS-treated group, which was potentially related to the compromised protective mechanism of myocardial cells (Fig. 1G). IL-1 $\beta$  and TNF- $\alpha$  are key cytokines in the inflammatory response, and their increase is usually associated with exacerbation of inflammation and tissue damage. In terms of inflammatory factor expression, LPS treatment led to a significant increase in IL-1 $\beta$  and TNF- $\alpha$  mRNA expression levels, indicating an inflammatory response in myocardial cells, with severe inflammation at high dosages (Fig. 1H,I). The increase in serum LDH levels with increasing LPS dosage indicated myocardial cell damage and necrosis (Fig. 1J). In summary, LPS reduced cardiac pumping function by increasing the expression of inflammatory factors and causing myocardial cell damage. The decreased expression of SIRT3 may be associated with exacerbation of myocardial cell damage, whereas the increase in MITOL may be a cellular attempt to maintain mitochondrial function.

#### *SIRT3 Treatment Reduces LPS-Induced Myocardial Injury in Mice*

In normal mice, overexpression of SIRT3 (Control+OE-SIRT3) did not alter cardiac pumping function. However, LPS treatment reduced cardiac pumping function (LPS+OE-NC). Interestingly, overexpression of SIRT3 improved cardiac pumping function in the LPS-treated group (LPS+OE-SIRT3; Fig. 2A,B). Hematoxylin and eosin (HE) staining was used to assess the integrity of the myocardial tissue structure. The degree of myocardial injury was most severe in the LPS+OE-NC group, whereas overexpression of SIRT3

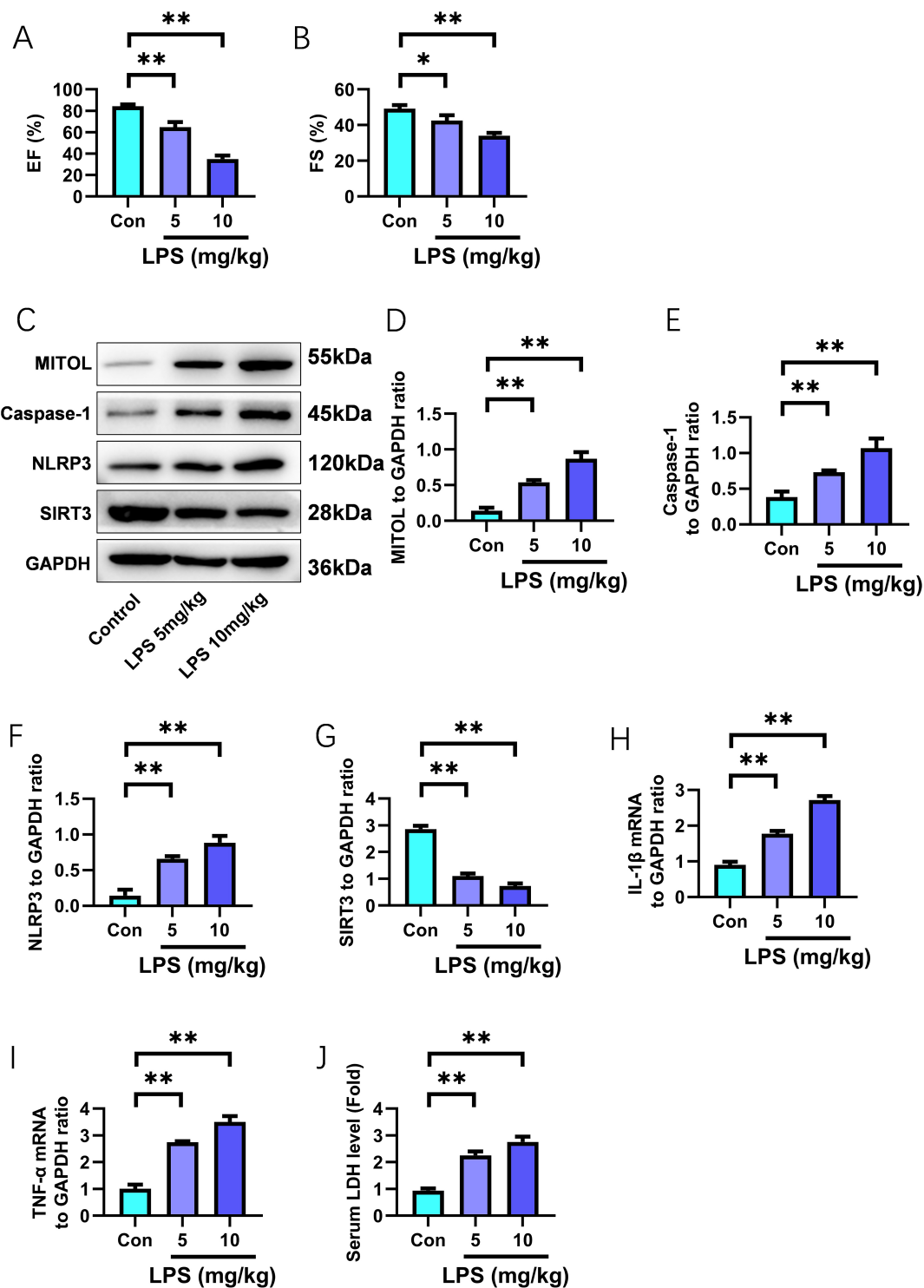


**Fig. 1. LPS-induced myocardial injury in mice.** (A) Left ventricular ejection fraction (LVEF). (B) Left ventricular fractional shortening (LVFS). (C–G) Expression levels of MITOL, Caspase-1, NLRP3, and SIRT3 in LPS-induced mice. (H,I) IL-1 $\beta$  (H) and TNF- $\alpha$  (I) mRNA expression in LPS-induced mice. (J) Serum levels of LDH in LPS-induced mice. \* $p < 0.05$ , \*\* $p < 0.01$ ,  $n = 6$ . IL-1 $\beta$ , Interleukin-1 beta; TNF- $\alpha$ , tumor necrosis factor-alpha; LDH, lactate dehydrogenase; LPS, lipopolysaccharide.

(Control+OE-SIRT3 and LPS+OE-SIRT3) significantly alleviated myocardial injury (Fig. 2C). SIRT3 expression was significantly higher in the Control+OE-SIRT3 group than in the Control+OE-NC group, indicating successful

overexpression. LPS treatment reduced the expression of SIRT3 (LPS+OE-NC), whereas overexpression of SIRT3 (LPS+OE-SIRT3) partially reversed this downward trend (Fig. 2D,E). In the LPS+OE-NC group, MITOL expression

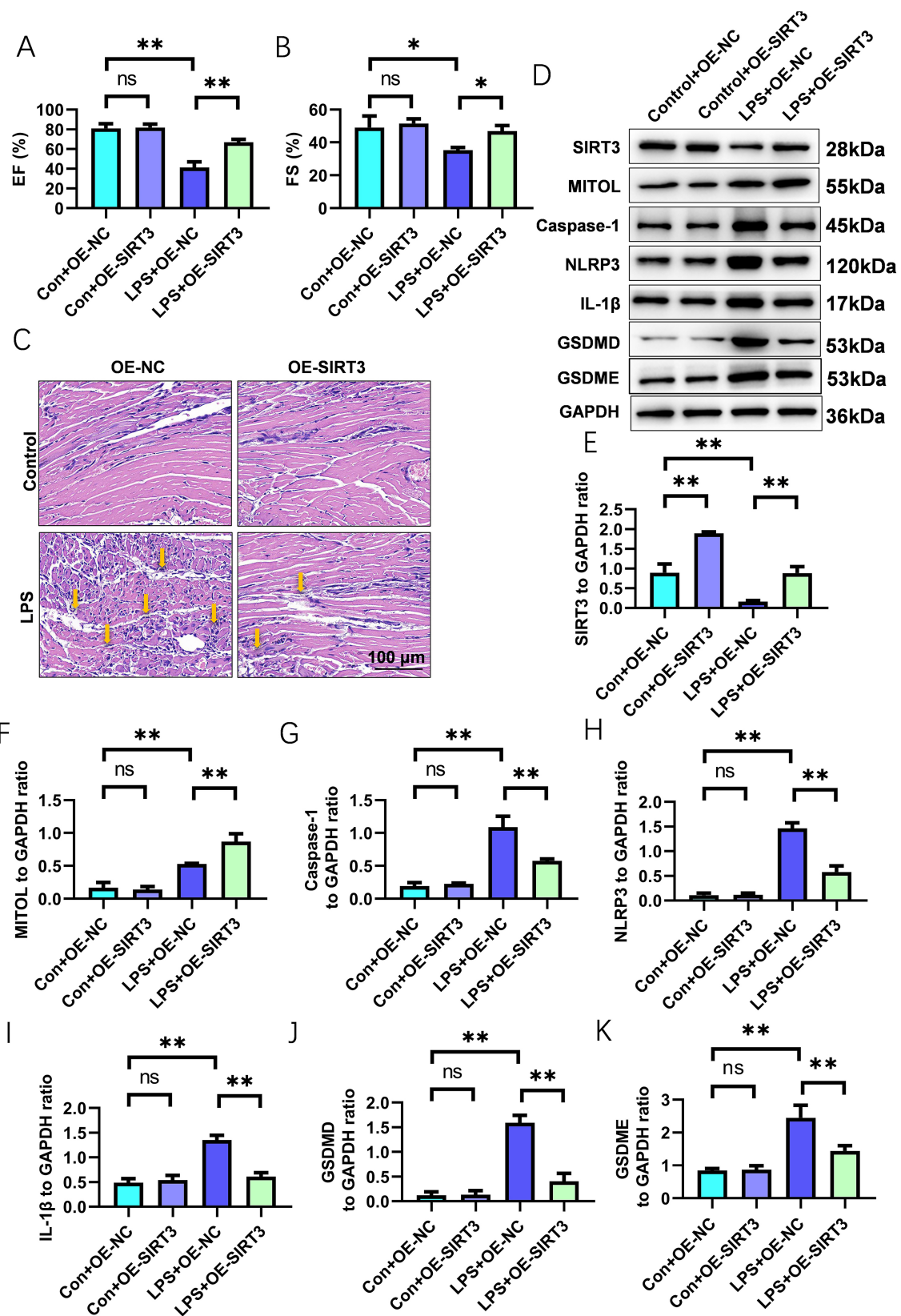


**Fig. 2. Overexpression of SIRT3 reduces LPS-induced myocardial injury.** (A) Left ventricular ejection fraction (LVEF). (B) Left ventricular fractional shortening (LVFS). (C) Representative images of HE-stained myocardial tissue. Yellow arrows represent the areas of tissue damage. (D–J) Expression levels of SIRT3 (E), MITOL (F), Caspase-1 (G), NLRP3 (H), IL-1β (I), GSDMD (J), and GSDME (K) in LPS-induced mice. ns, not significant, \* $p < 0.05$ , \*\* $p < 0.01$ ,  $n = 6$ .

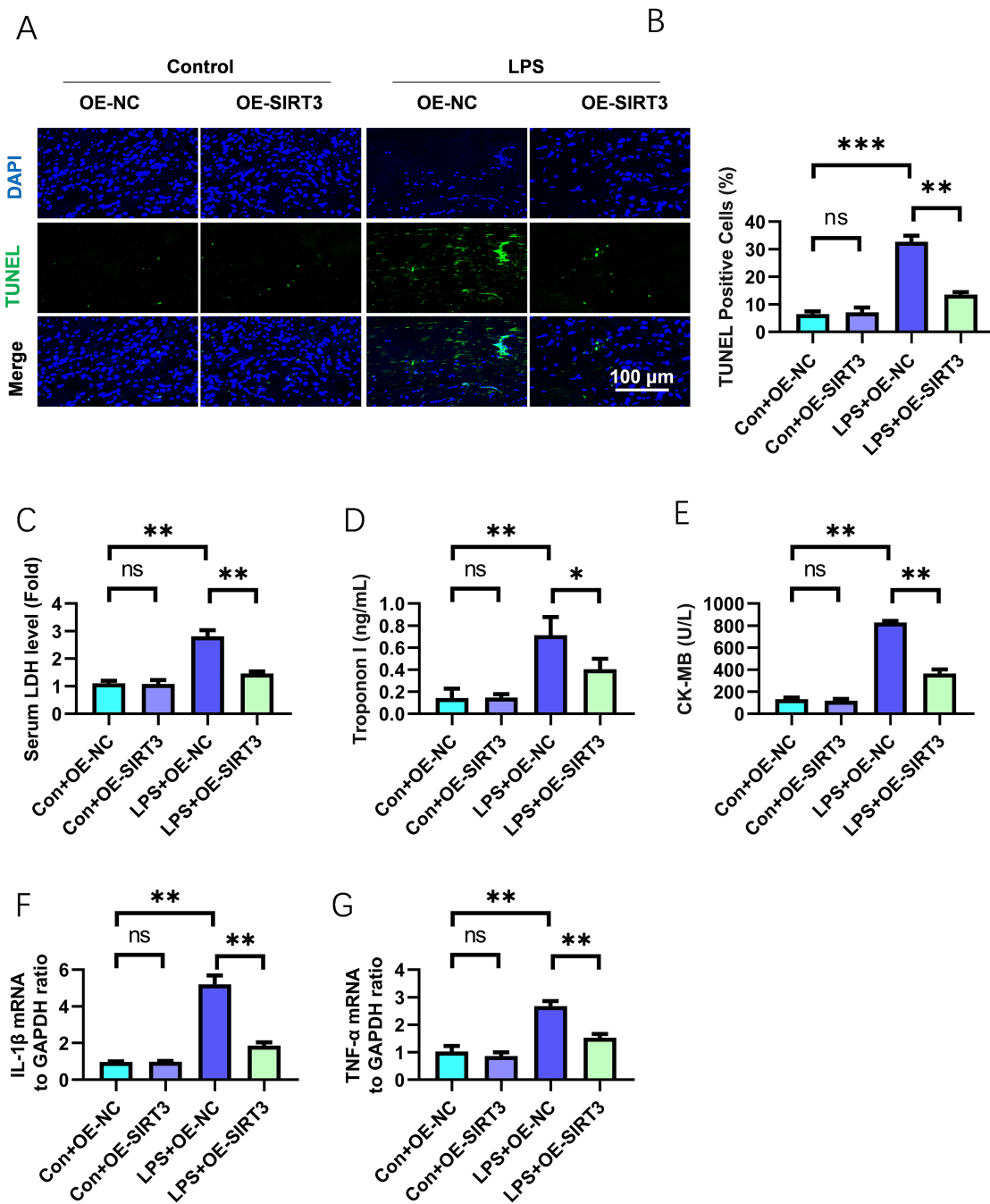


**Fig. 3. Effects of SIRT3 treatment on LPS-induced myocardial apoptosis, serum markers, and inflammatory factor expression in mice.** (A) Representative images of TUNEL staining. TUNEL-positive: Red fluorescence representing apoptosis. (B) Quantitative analysis of myocardial TUNEL staining. (C–E) Serum levels of LDH (C), cardiac troponin I (D), and CK-MB (E) in LPS-induced mice. (F,G) Expression levels of IL-1 $\beta$  (F) and TNF- $\alpha$  (G) detected by PCR. ns, not significant, \* $p < 0.05$ , \*\* $p < 0.01$ ,  $n = 6$ . TUNEL, terminal deoxynucleotidyl transferase dUTP nick end labeling; CK-MB, creatine kinase-MB; PCR, polymerase chain reaction.

increased, indicating increased mitochondrial stress. Overexpression of SIRT3 (LPS+OE-SIRT3) further increased MITOL expression, possibly to counteract LPS-induced mitochondrial damage (Fig. 2F). For Caspase-1, NLRP3, IL-1 $\beta$ , GSDMD, and GSDME, the expression of these inflammatory and apoptosis-related proteins significantly

increased in the LPS+OE-NC group, indicating that LPS induced inflammation and pyroptosis in myocardial cells. Overexpression of SIRT3 (LPS+OE-SIRT3) reduced the expression of these proteins, demonstrating the protective effect of SIRT3 (Fig. 2G–K).

### ***Therapeutic Effect of SIRT3 on LPS-Induced Myocardial Pyroptosis and Inflammatory Response in Mice***

TUNEL staining results showed that the number of apoptotic myocardial cells was low in the control groups (Control+OE-NC and Control+OE-SIRT3), and we found no significant difference between the two groups, indicating that overexpression of SIRT3 itself did not affect apoptosis. The number of apoptotic myocardial cells in the LPS-treated group (LPS+OE-NC) significantly increased, indicating that LPS induced apoptosis in myocardial cells. However, in the LPS-treated group with SIRT3 overexpression (LPS+OE-SIRT3), the number of apoptotic myocardial cells decreased significantly, indicating that overexpression of SIRT3 alleviated LPS-induced myocardial cell apoptosis (Fig. 3A,B). The levels of LDH, cardiac troponin I, and CK-MB in the control group were low, and overexpression of SIRT3 did not change these indicators. LPS treatment significantly increased the levels of these serum indicators, indicating myocardial injury. In the LPS-treated group with SIRT3 overexpression (LPS+OE-SIRT3), the levels of these indicators were lower than those in the LPS+OE-NC group, indicating that overexpression of SIRT3 helped alleviate LPS-induced myocardial injury (Fig. 3C–E). IL-1 $\beta$  and TNF- $\alpha$  were low in the control group, whereas LPS treatment significantly increased the expression of these inflammatory factors, indicating a strong inflammatory response induced by LPS. Compared with the LPS+OE-NC group, IL-1 $\beta$  and TNF- $\alpha$  in the LPS+OE-SIRT3 group were reduced, indicating that overexpression of SIRT3 could alleviate the LPS-induced inflammatory response (Fig. 3F,G).

### ***Therapeutic Effect of SIRT3 on LPS-Induced Myocardial Pyroptosis in H9C2 Cells***

The number of EdU-positive cells in the control groups (Control+OE-NC and Control+OE-SIRT3) was the same, indicating that overexpression of SIRT3 itself did not affect cell viability. Cell viability in the LPS-treated group (LPS+OE-NC) was the lowest, indicating that LPS significantly reduced cell viability. Cell viability in the LPS-treated group with SIRT3 overexpression (LPS+OE-SIRT3) was higher than that in the group treated with LPS alone, suggesting that overexpression of SIRT3 could improve cell viability after LPS treatment (Fig. 4A). The expression of MITOL remained unchanged in the control group, but it significantly increased in the LPS-treated group, especially in the LPS-treated group with SIRT3 overexpression (LPS+OE-SIRT3). Thus, SIRT3 may act by increasing the expression of MITOL (Fig. 4B,C). Caspase-1, NLRP3, IL-1 $\beta$ , GSDMD, and GSDME were expressed at low levels in the control group and significantly increased in the LPS-treated group. However, in the LPS-treated group with SIRT3 overexpression, these pyroptosis-related proteins decreased, indicating that overexpression of SIRT3

may alleviate cell pyroptosis and inflammatory response by reducing the expression of these proteins (Fig. 4D–H). IL-1 $\beta$  and TNF- $\alpha$  were low in the control group, which meant the absence of an inflammatory response. After LPS treatment, IL-1 $\beta$  and TNF- $\alpha$  significantly increased, indicating an LPS-induced inflammatory response. In the LPS-treated group with SIRT3 overexpression, IL-1 $\beta$  and TNF- $\alpha$  were lower than those in the group treated with LPS alone. Thus, overexpression of SIRT3 could alleviate the LPS-induced inflammatory response (Fig. 4I,J).

### ***Silencing MITOL Reverses the Therapeutic Effect of SIRT3 on Myocardial Cell Injury***

The expression level of MITOL in the siNC group, used as a control, was relatively high. The expression of MITOL in the siMITOL-1 group decreased the most, indicating a significant silencing effect. The silencing effect of siMITOL-2 was not as effective as that of siMITOL-1; therefore, siMITOL-1 was used for subsequent experiments (Fig. 5A). Levels of ROS were detected by DCFH-DA fluorescence assay. The results showed that the control group (Control) had the lowest ROS levels. The group overexpressing SIRT3 (LPS+OE-SIRT3) had higher ROS levels than the control group, indicating that SIRT3 overexpression may reduce ROS production under LPS stimulation. The LPS-treated group (LPS+NC) and the SIRT3 overexpression group with silenced MITOL (LPS+OE-SIRT3+siMITOL) had the same and highest ROS levels. This result demonstrated that silencing MITOL reversed the protective effect of SIRT3, leading to an increase in ROS levels to the same level as LPS treatment alone (Fig. 5B). The control group (Control) had the highest JC-1 aggregate/monomer ratio, indicating normal mitochondrial function. The group overexpressing SIRT3 (LPS+OE-SIRT3) had a lower ratio than the control group; thus, SIRT3 overexpression improved mitochondrial function but was still affected by LPS. The LPS-treated group (LPS+NC) and the SIRT3 overexpression group with silenced MITOL (LPS+OE-SIRT3+siMITOL) had the lowest and equal ratios, indicating severe mitochondrial dysfunction; silencing MITOL reversed the protective effect of SIRT3 (Fig. 5C). The control group (Control) had the fewest pyroptotic bodies, with intact cell structure. The group overexpressing SIRT3 (LPS+OE-SIRT3) had an intermediate number of pyroptotic bodies between the control group and the LPS-treated group, indicating a protective effect of SIRT3 overexpression. The LPS-treated group (LPS+NC) and the SIRT3 overexpression group with silenced MITOL (LPS+OE-SIRT3+siMITOL) had the most and equal number of pyroptotic bodies, indicating complete reversal of the protective effect of SIRT3 by silencing MITOL, with the extent of cell pyroptosis similar to LPS treatment alone (Fig. 5D). These experimental results indicated that SIRT3 alleviated LPS-induced myocardial cell injury through a

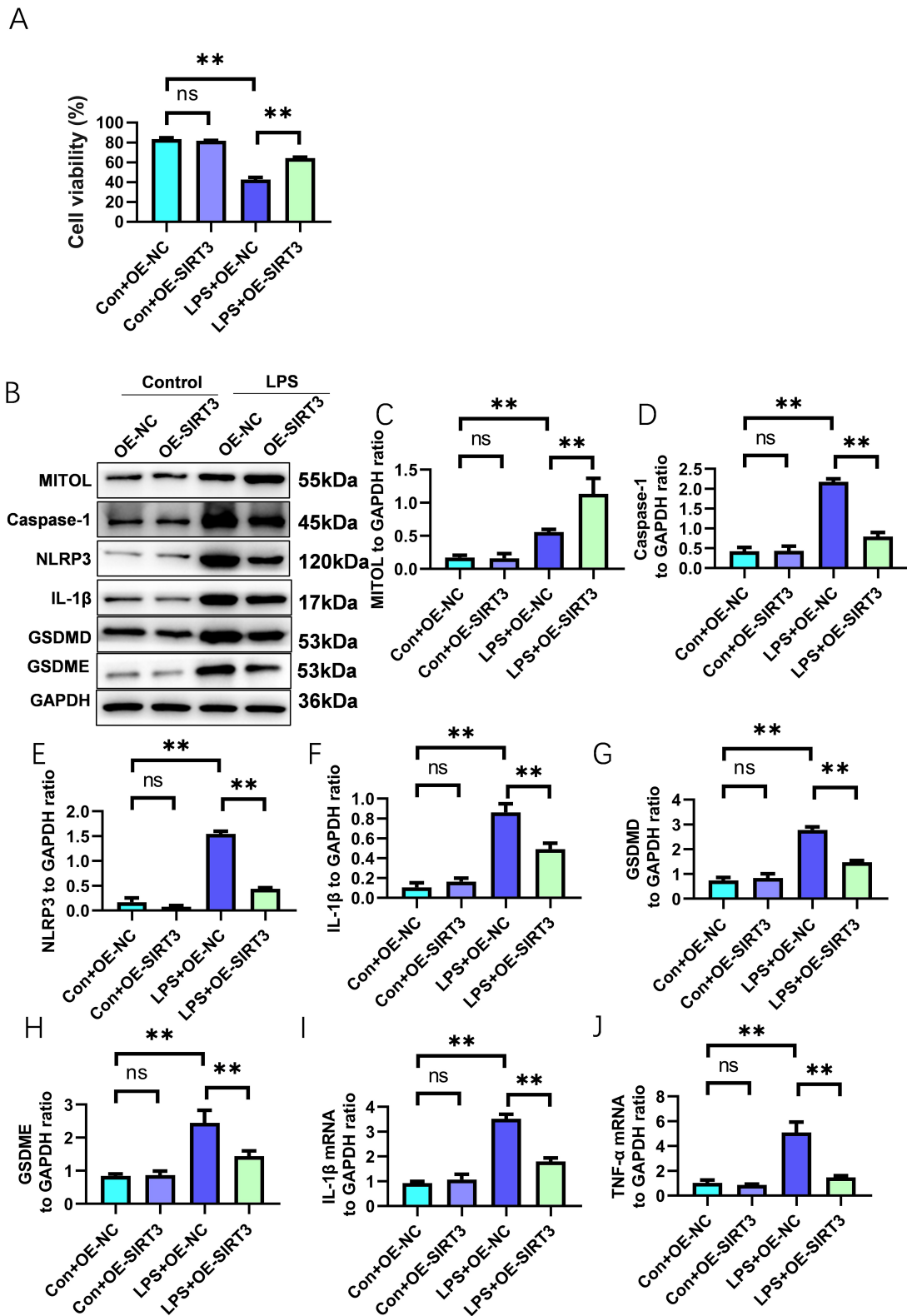


**Fig. 4.** Effects of SIRT3 treatment on the expression of MITOL and pyroptosis-related proteins in LPS-induced H9C2 cells. (A) CCK-8 assay to assess cell viability. (B) Representative immunoblot images of SIRT3 treatment in LPS-induced H9C2 cells. (C–G) Expression levels of MITOL (C), Caspase-1 (D), NLRP3 (E), IL-1 $\beta$  (F), GSDMD (G), and GSDME (H) in LPS-induced mice. (I, J) Expression levels of IL-1 $\beta$  (I) and TNF- $\alpha$  (J) detected by PCR. ns, not significant, \*\* $p < 0.01$ ,  $n = 3$ .

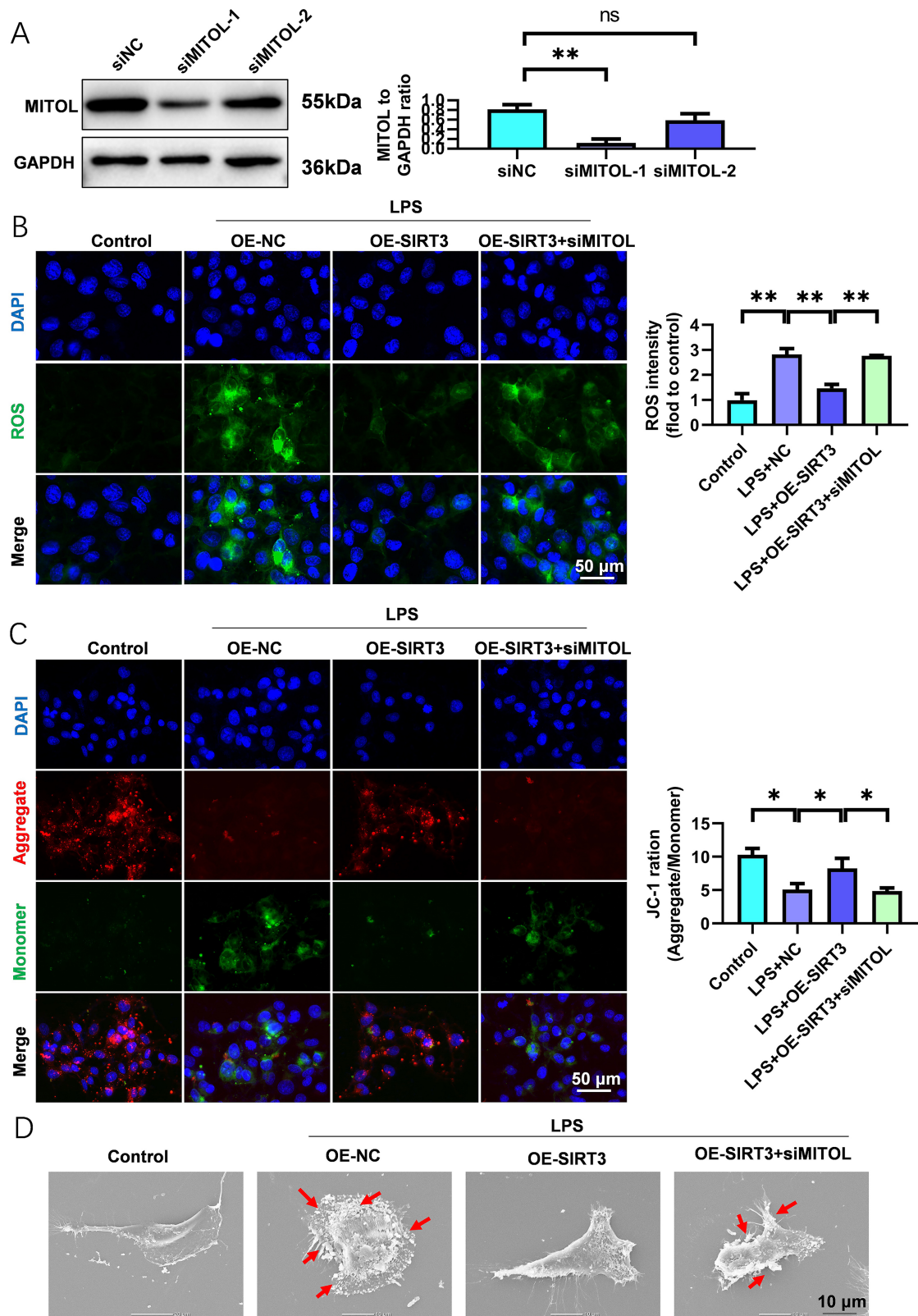


**Fig. 5. Reversal of the therapeutic effect of SIRT3 on myocardial cell injury by MITOL silencing.** (A) Detection of MITOL silencing transfection efficiency in H9C2 cells. (B) ROS levels detected by DCFH-DA fluorescence. (C) Fluorescence images of JC-1 aggregates/monomers in H9C2 cells. (D) Scanning electron microscopy experiment to detect the reversal of the protective effect of SIRT3 by MITOL silencing. ns, not significant, \* $p < 0.05$ , \*\* $p < 0.01$ ,  $n = 3$ .

MITOL-dependent mechanism, which was reversed upon silencing MITOL. SIRT3 overexpression reduced ROS levels, improved mitochondrial function, and reduced the formation of pyroptotic bodies, all of which were lost upon silencing MITOL. These findings highlighted the important role of MITOL in the SIRT3-mediated myocardial cell protection mechanism.

## Discussion

Myocardial inflammation and the associated pyroptosis of myocardial cells are key driving factors in various cardiac pathological states, especially in the context of infection and sepsis [22,23]. This study analyzed the role of SIRT3, a mitochondrial NAD<sup>+</sup>-dependent deacetylase, in regulating the inflammatory response and cell pyroptosis in the myocardium, as well as the potential role of MITOL in this process. The study primarily found that overexpression of SIRT3 significantly reduced the pyroptosis rate of myocardial cells treated with LPS. The cardioprotective effect mediated by SIRT3 was closely associated with its regulation of MITOL expression and activity. Silencing of MITOL reversed the protective effect of SIRT3 on myocardial cells, indicating that MITOL is a necessary mediator for the action of SIRT3.

Previous studies have shown that SIRT3 can protect myocardial cells by regulating the oxidative stress response and mitochondrial function [24–26]. Our results further confirmed the critical role of SIRT3 in protecting myocardial cells and revealed a new mechanism by which it inhibited LPS-induced myocardial cell pyroptosis through the regulation of MITOL. The role of SIRT3 as a mitochondrial protective factor has been gradually confirmed in recent research. The experimental results of this study also found that SIRT3 treatment significantly reduced LPS-induced myocardial injury. This therapeutic effect was not only reflected in the improvement of cardiac function but also involved the downregulation of markers of myocardial cell pyroptosis, including decreased expression of pyroptosis-related proteins and reduced expression of the inflammatory factors TNF $\alpha$  and IL-1 $\beta$ . These findings emphasize the dual role of SIRT3 in anti-inflammation and anti-myocardial cell pyroptosis. Further cellular level experiments revealed the molecular mechanism of SIRT3's protective effect on myocardial cells. SIRT3 treatment can promote the survival of H9C2 myocardial cells and reduce LPS-induced myocardial cell pyroptosis. These effects are closely related to changes in MITOL expression and pyroptosis-related protein expression. MITOL, as a mitochondrial ubiquitin ligase, has been increasingly recognized for its role in regulating mitochondrial quality control and cell death. Finally, we revealed that silencing MITOL could reverse the cardioprotective effect of SIRT3. This finding provides direct evidence of the interaction between

SIRT3 and MITOL and reveals the necessity of MITOL in SIRT3-mediated myocardial protection. Thus, SIRT3 may exert its effects by directly or indirectly regulating the activity or expression of MITOL, influencing the survival and death of myocardial cells.

The interaction between SIRT3 and MITOL is a novel finding of this study. Previous research largely focused on the activation of antioxidant enzymes by SIRT3 [16,27], with relatively few studies on how SIRT3 regulates the fate of myocardial cells through mitochondrial ubiquitin ligase. Our study fills this gap and provides new insights into the interaction of SIRT3 and MITOL in cardiac protection. Another important finding of this study is the necessity of MITOL in SIRT3-mediated myocardial protection. Although the role of MITOL in regulating mitochondrial quality and cell death has been gaining attention [7,28], its specific function in myocardial cells remains unclear. Our study suggested that MITOL is an important downstream molecule for SIRT3-mediated cardiac protection, laying the foundation for further research into the role of MITOL in cardiac pathology.

Despite the achievements of our study, it had some limitations. This study was mainly conducted in cellular and animal models, and the interaction between SIRT3 and MITOL and their role in cardiac protection has not been validated in clinical specimens. Future research should validate the biological significance of these findings. Additionally, the specific mechanism of action of MITOL and its detailed pathways in regulating myocardial cell pyroptosis are unclear and require further exploration. Furthermore, we should consider that SIRT3 may have other unknown downstream effectors that may play a role in cardiac protection. Future research should also explore how to modulate the activity of SIRT3 and MITOL through drugs or other interventions for the treatment of heart disease.

## Conclusion

In summary, our study revealed the important role of SIRT3 in inhibiting myocardial inflammation and pyroptosis and highlighted the importance of MITOL as its downstream effector. These findings provide new perspectives for future cardiology research and may offer new strategies for the treatment of inflammation-related myocardial injury. Future research needs to explore the specific interaction mechanisms between SIRT3 and MITOL, as well as their roles and potential clinical applications in cardiac pathology.

## Availability of Data and Materials

The original contributions presented in the study are included in the article/supplementary material. Further inquiries can be directed to the corresponding authors.

## Author Contributions

PL: Conception, Design, Materials, Data Collection, Analysis, Literature Review, and Writing. LW: Design, Supervision, Materials, Data Collection, Analysis, Literature Review, and Writing. Both authors contributed to editorial changes in the manuscript. Both authors read and approved the final manuscript. Both authors have participated sufficiently in the work to take public responsibility for appropriate portions of the content and agreed to be accountable for all aspects of the work in ensuring that questions related to its accuracy or integrity.

## Ethics Approval and Consent to Participate

This study has been approved by Zhang Ye People's Hospital affiliated to Hexi University. Approval No.: ZYAF/SQ-02/02.1.

## Acknowledgment

Not applicable.

## Funding

This research was funded by Gansu Provincial Natural Science Foundation (Project No.: 23JRRG0011).

## Conflict of Interest

The authors declare no conflict of interest.

## References

- [1] Lafuse WP, Wozniak DJ, Rajaram MVS. Role of Cardiac Macrophages on Cardiac Inflammation, Fibrosis and Tissue Repair. *Cells*. 2020; 10: 51.
- [2] Lawler PR, Bhatt DL, Godoy LC, Lüscher TF, Bonow RO, Verma S, *et al.* Targeting cardiovascular inflammation: next steps in clinical translation. *European Heart Journal*. 2021; 42: 113–131.
- [3] Alfaddagh A, Martin SS, Leucker TM, Michos ED, Blaha MJ, Lowenstein CJ, *et al.* Inflammation and cardiovascular disease: From mechanisms to therapeutics. *American Journal of Preventive Cardiology*. 2020; 4: 100130.
- [4] Palomer X, Román-Azcona MS, Pizarro-Delgado J, Planavila A, Villarroya F, Valenzuela-Alcaraz B, *et al.* SIRT3-mediated inhibition of FOS through histone H3 deacetylation prevents cardiac fibrosis and inflammation. *Signal Transduction and Targeted Therapy*. 2020; 5: 14.
- [5] Guo X, Yan F, Li J, Zhang C, Su H, Bu P. SIRT3 Ablation Deteriorates Obesity-Related Cardiac Remodeling by Modulating ROS-NF- $\kappa$ B-MCP-1 Signaling Pathway. *Journal of Cardiovascular Pharmacology*. 2020; 76: 296–304.
- [6] Dikalova AE, Pandey A, Xiao L, Arslanbaeva L, Sidorova T, Lopez MG, *et al.* Mitochondrial Deacetylase Sirt3 Reduces Vascular Dysfunction and Hypertension While Sirt3 Depletion in Essential Hypertension Is Linked to Vascular Inflammation and Oxidative Stress. *Circulation Research*. 2020; 126: 439–452.
- [7] Shiiba I, Takeda K, Nagashima S, Yanagi S. Overview of Mitochondrial E3 Ubiquitin Ligase MITOL/MARCH5 from Molecular Mechanisms to Diseases. *International Journal of Molecular Sciences*. 2020; 21: 3781.
- [8] Takeda K, Uda A, Mitsubori M, Nagashima S, Iwasaki H, Ito N, *et al.* Mitochondrial ubiquitin ligase alleviates Alzheimer's disease pathology via blocking the toxic amyloid- $\beta$  oligomer generation. *Communications Biology*. 2021; 4: 192.
- [9] Lu L, Ma J, Tang J, Liu Y, Zheng Q, Chen S, *et al.* Irisin attenuates myocardial ischemia/reperfusion-induced cardiac dysfunction by regulating ER-mitochondria interaction through a mitochondrial ubiquitin ligase-dependent mechanism. *Clinical and Translational Medicine*. 2020; 10: e166.
- [10] Schirmacher V. Mitochondria at Work: New Insights into Regulation and Dysregulation of Cellular Energy Supply and Metabolism. *Biomedicine*. 2020; 8: 526.
- [11] Abate M, Festa A, Falco M, Lombardi A, Luce A, Grimaldi A, *et al.* Mitochondria as playmakers of apoptosis, autophagy and senescence. *Seminars in Cell & Developmental Biology*. 2020; 98: 139–153.
- [12] Wang Y, Li X, Zhao F. MCU-Dependent mROS Generation Regulates Cell Metabolism and Cell Death Modulated by the AMPK/PGC-1 $\alpha$ /SIRT3 Signaling Pathway. *Frontiers in Medicine*. 2021; 8: 674986.
- [13] Yapryntseva MA, Maximchik PV, Zhivotovsky B, Gogvadze V. Mitochondrial sirtuin 3 and various cell death modalities. *Frontiers in Cell and Developmental Biology*. 2022; 10: 947357.
- [14] Shen Y, Wu Q, Shi J, Zhou S. Regulation of SIRT3 on mitochondrial functions and oxidative stress in Parkinson's disease. *Biomedicine & Pharmacotherapy = Biomedecine & Pharmacotherapie*. 2020; 132: 110928.
- [15] Qiu X, Brown K, Hirsche MD, Verdin E, Chen D. Calorie restriction reduces oxidative stress by SIRT3-mediated SOD2 activation. *Cell Metabolism*. 2010; 12: 662–667.
- [16] Tao R, Vassilopoulos A, Parisiadou L, Yan Y, Gius D. Regulation of MnSOD enzymatic activity by Sirt3 connects the mitochondrial acetylation signaling networks to aging and carcinogenesis. *Antioxidants & Redox Signaling*. 2014; 20: 1646–1654.
- [17] Chapman J, Ng YS, Nicholls TJ. The Maintenance of Mitochondrial DNA Integrity and Dynamics by Mitochondrial Membranes. *Life (Basel, Switzerland)*. 2020; 10: 164.
- [18] Pickles S, Vigié P, Youle RJ. Mitophagy and Quality Control Mechanisms in Mitochondrial Maintenance. *Current Biology*. 2018; 28: R170–R185.
- [19] Nagashima S, Tokuyama T, Yonashiro R, Inatome R, Yanagi S. Roles of mitochondrial ubiquitin ligase MITOL/MARCH5 in mitochondrial dynamics and diseases. *Journal of Biochemistry*. 2014; 155: 273–279.
- [20] Yonashiro R, Ishido S, Kyo S, Fukuda T, Goto E, Matsuki Y, *et al.* A novel mitochondrial ubiquitin ligase plays a critical role in mitochondrial dynamics. *The EMBO Journal*. 2006; 25: 3618–3626.
- [21] Li N, Wang W, Zhou H, Wu Q, Duan M, Liu C, *et al.* Ferritinophagy-mediated ferroptosis is involved in sepsis-induced cardiac injury. *Free Radical Biology & Medicine*. 2020; 160: 303–318.
- [22] Kakahana Y, Ito T, Nakahara M, Yamaguchi K, Yasuda T. Sepsis-induced myocardial dysfunction: pathophysiology and management. *Journal of Intensive Care*. 2016; 4: 22.
- [23] Li Y, Ge S, Peng Y, Chen X. Inflammation and cardiac dysfunction

- tion during sepsis, muscular dystrophy, and myocarditis. *Burns & Trauma*. 2013; 1: 109–121.
- [24] Chen CJ, Fu YC, Yu W, Wang W. SIRT3 protects cardiomyocytes from oxidative stress-mediated cell death by activating NF- $\kappa$ B. *Biochemical and Biophysical Research Communications*. 2013; 430: 798–803.
- [25] Zhai M, Li B, Duan W, Jing L, Zhang B, Zhang M, *et al*. Melatonin ameliorates myocardial ischemia reperfusion injury through SIRT3-dependent regulation of oxidative stress and apoptosis. *Journal of Pineal Research*. 2017; 63: 10.1111/jpi.12419.
- [26] Bugga P, Alam MJ, Kumar R, Pal S, Chattopadhyay N, Banerjee SK. Sirt3 ameliorates mitochondrial dysfunction and oxidative stress through regulating mitochondrial biogenesis and dynamics in cardiomyoblast. *Cellular Signalling*. 2022; 94: 110309.
- [27] Gounden S, Phulukdaree A, Moodley D, Chaturgoon A. Increased SIRT3 Expression and Antioxidant Defense under Hyperglycemic Conditions in HepG2 Cells. *Metabolic Syndrome and Related Disorders*. 2015; 13: 255–263.
- [28] Giacomello M, Pellegrini L. The coming of age of the mitochondria-ER contact: a matter of thickness. *Cell Death and Differentiation*. 2016; 23: 1417–1427.